

How accurate is accurate enough for measuring sea-level rise and variability

Received: 10 November 2022

Accepted: 20 June 2023

Published online: 3 August 2023

 Check for updates

Benoit Meyssignac^{1,2}✉, **Michael Ablain**^{3,10}, **Adrien Guérou**^{4,10}, **Pierre Prandi**^{4,10}, **Anne Barnoud**³, **Alejandro Blazquez**^{1,2}, **Sébastien Fourest**^{1,2}, **Victor Rousseau**³, **Pascal Bonnefond**⁵, **Anny Cazenave**^{1,2}, **Jonathan Chenal**⁶, **Gerald Dibarboure**², **Craig Donlon**⁷, **Jérôme Benveniste**⁸, **Annick Sylvestre-Baron**² & **Nadya Vinogradova**⁹

Sea-level measurements from radar satellite altimetry have reached a high level of accuracy and precision, which enables detection of global mean sea-level rise and attribution of most of the rate of rise to greenhouse gas emissions. This achievement is far beyond the original objectives of satellite altimetry missions. However, recent research shows that there is still room for improving the performance of satellite altimetry. Reduced uncertainties would enable regionalization of the detection and attribution of the anthropogenic signal in sea-level rise and provide new observational constraints on the water–energy cycle response to greenhouse gas emissions by improving the estimate of the ocean heat uptake and the Earth energy imbalance.

Sea-level estimates derived from high-precision satellite altimetry measurements have now reached a level of maturity that is unprecedented. Among the essential climate variables that are routinely monitored, sea level is arguably one of the most advanced, with quasi-global coverage, a very low ratio of missing or corrupted data (<4%), an advanced estimate of the uncertainties at global and local scales that accounts for the time correlation in errors, and robust validation through both comparisons with tide gauge records and regular assessments of closure of the sea-level budget¹. Sea-level data quality is evaluated by a detailed analysis of the altimetry measurement uncertainty budget, and it shows a very low uncertainty level (for example, $\pm 0.3 \text{ mm yr}^{-1}$ in 20 yr and longer trends) that exceeds the altimetry missions' requirements². This low level of uncertainty raises the question of whether there is a need of further research to improve the sea-level record. Simply put, the question is: how accurate is accurate enough? This question is important for the ocean surface and topography science community and the general ocean science community, as an important amount of resources is currently used to continuously refine and improve knowledge of the sea-level record uncertainty.

Here we explore the uncertainty that should be targeted by future satellite altimetry constellations for global mean and regional sea-level estimates. We review the literature and find that three major science questions still need an improved sea-level measurement performance that is higher than currently available from satellite altimetry systems today. First, can improvements close the sea-level budget? Second, is it possible to detect and attribute the signal in sea level that is forced by GHG emissions? Third, will this allow estimation of the current Earth energy imbalance (EEI) mean and variability? Although the uncertainty of satellite altimetry measurements is close to the limits of the current capacity of the altimetry system, we argue that there is still room for improvement. Improved performance would bring important insights on the three science questions, particularly at large spatial scales (>1,000 km). However, locally, at smaller scales, spatially random errors do not average out, and the level of uncertainty is too high to expect to tackle the three science questions. To meet regional-scale requirements, important changes to the altimetry system would be needed, such as better long-term measurement stability of wet tropospheric delay derived from microwave radiometer instruments

¹LEGOS, CNES, CNRS, IRD, Université Paul Sabatier, Toulouse, France. ²CNES, Toulouse, France. ³Magellium, Ramonville Saint-Agne, France. ⁴CLS, Ramonville Saint-Agne, France. ⁵SYRTE, Observatoire de Paris, PSL Research University, CNRS, Sorbonne Universités, UPMC Univ. Paris 06, LNE, Paris, France. ⁶Direction des Programmes, IGN, Ramonville-Saint-Agne, France. ⁷ESTEC, ESA, Noordwijk, the Netherlands. ⁸ESRIN, ESA, Frascati, Italy. ⁹Science Mission Directorate, NASA, Washington, DC, US. ¹⁰These authors contributed equally: Michael Ablain, Adrien Guérou, Pierre Prandi.

✉ e-mail: benoit.meyssignac@univ-tlse3.fr

(for example, by improving their calibration strategy) or improvement of the International Terrestrial Reference Frame (ITRF) realization accuracy. (Note that the terms ‘accuracy’, ‘precision’ and ‘uncertainty’ can have different meanings in different science communities. To avoid any confusion, in this Perspective we use the metrology definition of these terms given by the Bureau International des Poids et Mesures³.)

Accuracy and precision of the current sea-level observing system

In August 1992, the launch of the TOPEX/Poseidon mission, jointly developed by the National Aeronautics and Space Administration and the Centre National d’Etudes Spatiales, was a milestone in the development of the satellite altimetry observing system that began a new era in oceanography and sea-level science⁴. The use of an on-board microwave radiometer to measure the atmospheric water content along the same path as the radar signal (hence to precisely estimate the delay caused on it by tropospheric water vapour) as well as precise orbit tracking by different instruments (GNSS, DORIS and laser ranging instruments) drastically increased the accuracy of the orbit determination and range measurement (that is, the distance between the spacecraft and the ocean surface) compared with earlier missions^{5,6}. For the first time, it became possible to remotely measure absolute sea-level changes in the ITRF with an accuracy of a few centimetres, on a global basis, every ten days. Ocean tides and large-scale geostrophic circulation were suddenly readily observable over the global ocean, rapidly leading to major progress in oceanography^{6–8}. After a few years, TOPEX/Poseidon revealed oceanic signals on spatial scales much smaller than 1,000 km. At larger spatial scales, the random noise averages out, revealing signals of a few millimetres in amplitude such as the asymmetric seasonal cycle in sea level^{7,9}, the interannual variability of sea level in response to major climate modes of variability such as the El Niño–Southern Oscillation^{10–13}, the reduction of sea level in response to major volcanic eruptions^{14–16} and a persistent increase in global mean sea level (GMSL) of 3 to 4 mm yr⁻¹ (ref. 17; Fig. 1).

These millimetre-level signals on annual and longer timescales are caused by exchanges of heat and water between the ocean on one side and the atmosphere, the cryosphere and terrestrial waters on the other side^{18–22}. For example, when the ocean absorbs 0.1 W m⁻² of heat, the ocean water expands, and GMSL rises by 0.24 mm yr⁻¹; or when 100 Gt of land water (in the form of melted ice or liquid water) runs off to the ocean, the ocean mass increases, and GMSL rises by 0.27 mm yr⁻¹ (Table 1). By monitoring such small signals, satellite altimetry enabled researchers for the first time to quantify (either directly or through reanalysis) the response of sea level to changes in the global Earth energy cycle and water cycle.

During the 2000s, two other key improvements in the ocean observing system were achieved with the implementation of the global Argo array of autonomous profiling floats (the Argo project²³) and the launch of the Gravity Recovery and Climate Experiment (GRACE) mission²⁴. The Argo array allowed, for the first time, the continuous monitoring of the temperature and salinity of the upper 2,000 m of the ocean, with quasi-global coverage and with high precision and accuracy (± 0.002 K in temperature and ± 2.4 dbar in pressure, for example²⁵) controlled through validation against conductivity–temperature–depth systems²⁶. Although the Argo array is not very dense (it consists of a few thousands of point-wise profiler measurements), it reached sufficient spatial sampling in 2005 to yield an improved measure of the global thermal expansion of the ocean²⁷ and quantify the amount of global sea-level change that was caused by the ocean heat content change (Fig. 1). The space gravimetry GRACE mission delivered measurements of mass transfers at Earth’s surface on interannual timescales with unprecedented precision and accuracy²⁸. By 2004, the quality of GRACE data was sufficient to yield a measure of the ocean mass change and to quantify the amount of global sea-level change that was caused by land-ice loss and land water storage changes^{29–31} (Fig. 1). Since 2005, the availability of both Argo data and GRACE data allowed researchers

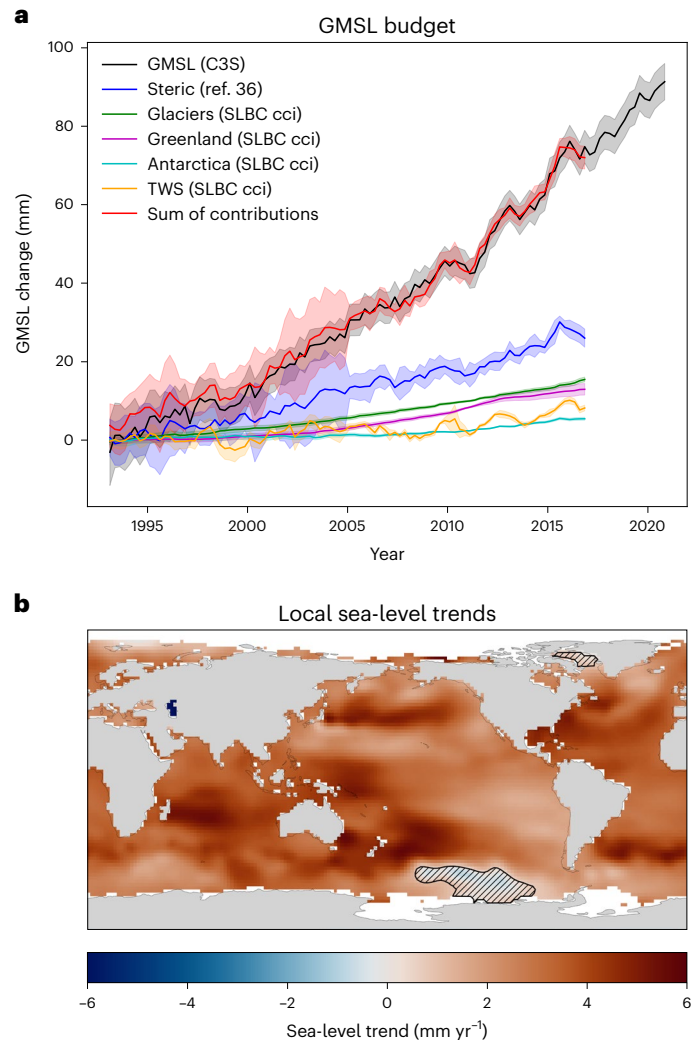


Fig. 1 | Sea-level changes. **a**, GMSL changes measured by satellite altimetry (black line) from the Copernicus Climate Change Service (C3S) v.DT2021 data⁹¹ with uncertainties at 10 days (5–95% CL, indicated by the black shaded area) and the different contributions to sea-level changes from the Sea Level Budget Closure climate change initiative (SLBC cci²²): thermal expansion³⁶ (blue line), glacier ice melt (green line), Greenland mass loss (pink line), Antarctica mass loss (cyan line) and land water storage variations (TWS, orange curve). The red line is the sum of the contributions to sea-level rise. **b**, Regional sea-level rates of rise over 1993–2019 estimated in ref. 50 (the hatched areas are regions where regional sea-level rates of rise are not significant at the 5–95% CL; see Fig. 2 for the uncertainties). The regional acceleration in sea-level rise is available in Supplementary Information (Supplementary Fig. 1).

to partition sea-level changes into thermal expansion and ocean mass changes and to verify (by comparing them with satellite altimetry data) that the sum of these contributions explains total sea-level changes within uncertainties^{17,18,32,33}. Since then, closing the sea-level budget at annual and longer timescales, at a useful level of accuracy and with useful confidence, became an essential and central problem of modern physical oceanography.

Closing the sea-level budget is essential for three reasons. First, closing the sea-level budget guarantees that all important causes of sea-level variability are identified and that their combination matches total sea-level changes. In other words, it is a means to ensure, with high confidence, a quantitative understanding of why and how the sea level is rising. Second, closing the sea-level budget is a tool to cross-validate worldwide complex observing systems such as the Argo network, the space gravimetry missions GRACE-GRACE-FO and the satellite altimetry

Table 1 | Oceanic heat uptake change or water transfer from the continents implied by a 1 mm yr⁻¹ rate of sea-level rise

GMSL rise	Equivalent global OHU	Equivalent mass transfer from the continents
1 mm yr ⁻¹ SLE	0.42 W m ⁻²	361.8 Gt yr ⁻¹

SLE, global mean sea-level equivalent.

system and to keep a close watch on their performance. Indeed, the built-in redundancy, which allows sea level to be monitored by two independent observing systems (satellite altimetry on one side and Argo plus GRACE on the other), is ideal for detecting occasional issues or long-term drifts in the instruments of each observing system^{21,34–37}. Third, closing the sea-level budget is an efficient approach to testing the consistency of different observed variables of the climate system including sea level, ocean temperature and ocean mass, with regard to conservation laws including those of mass, energy and freshwater. This consistency is crucial to using observed variables to test physical theories^{38,39} or to constrain dynamical state estimates from numerical models^{40,41}. This is particularly important for ocean reanalyses that need to assimilate coherent observed data to consistently constrain a large set of variables that are related and bound together by the equations of dynamics and thermodynamics⁴².

Today—that is, 30 years after the launch of TOPEX/Poseidon and more than 20 years after the launch of GRACE and the deployment of the Argo network—what is the current state of knowledge? Here we discuss whether there has been any progress in the resolution, accuracy and precision of satellite altimetry and whether the sea-level budget is being closed with lower uncertainty.

In total, 16 satellite altimeters have flown since TOPEX/Poseidon, including the Jason satellite series on the same orbit as TOPEX/Poseidon, the Sentinel 3A/B satellites of the European Copernicus programme⁴³ and the recently launched Sentinel-6 Michael Friele mission ensuring continuity of the Jason series⁴⁴, also part of the operational European Copernicus programme. New synthetic aperture radar techniques employed by Sentinel-3 and Sentinel-6 altimeters provide access to measurements with improved uncertainty and with higher (typically 300 m) along-track sampling compared with previous low-resolution mode systems. The combination of measurements of satellite missions simultaneously in orbit allows daily sea-level estimates with a resolution of 1/4° × 1/4° from 82° S to 82° N (except in regions covered by sea ice). Although sea-level dynamics are highly heterogeneous, the time and space sampling is enough to effectively resolve the GMSL dynamics on a weekly basis^{45,46} and the regional dynamics at timescales of 34 days and spatial scales from 100 km at high latitudes to 800 km at the Equator⁴⁷. For a single 1 Hz measurement, the precision is between ±2 cm and ±2.5 cm at the 90% confidence level (CL) (due to random measurement errors linked to the sea state, the effects of long-wave swell systems and how a radar pulse interacts with the ocean surface⁴⁸), and the accuracy is between ±2.5 cm and ±3.5 cm at the 90% CL (due to systematic error coming from essentially the orbit determination and the wet tropospheric correction (WTC), which accounts for the atmospheric water vapour delay on the range measurement²). On timescales longer than 1 s and spatial scales larger than the footprint of the radar echo (typically several kilometres for the TOPEX/Poseidon and Jason satellites but much less for synthetic aperture radar altimeters such as Sentinel-3 and Sentinel-6), measurement errors show an important correlation across time and space that is essential to evaluate the uncertainty in sea-level estimates at timescales longer than one year. The error and its temporal correlation have been modelled at local and global scales and on interannual to multi-decadal timescales (Fig. 2). The error variance–covariance matrix of satellite altimetry (which characterizes the temporal correlations in errors) is now available from 1993 to 2021 for the GMSL^{2,49} and for the 1/4° × 1/4° sea-level grids⁵⁰. The error variance–covariance matrix enables us to estimate the uncertainty in

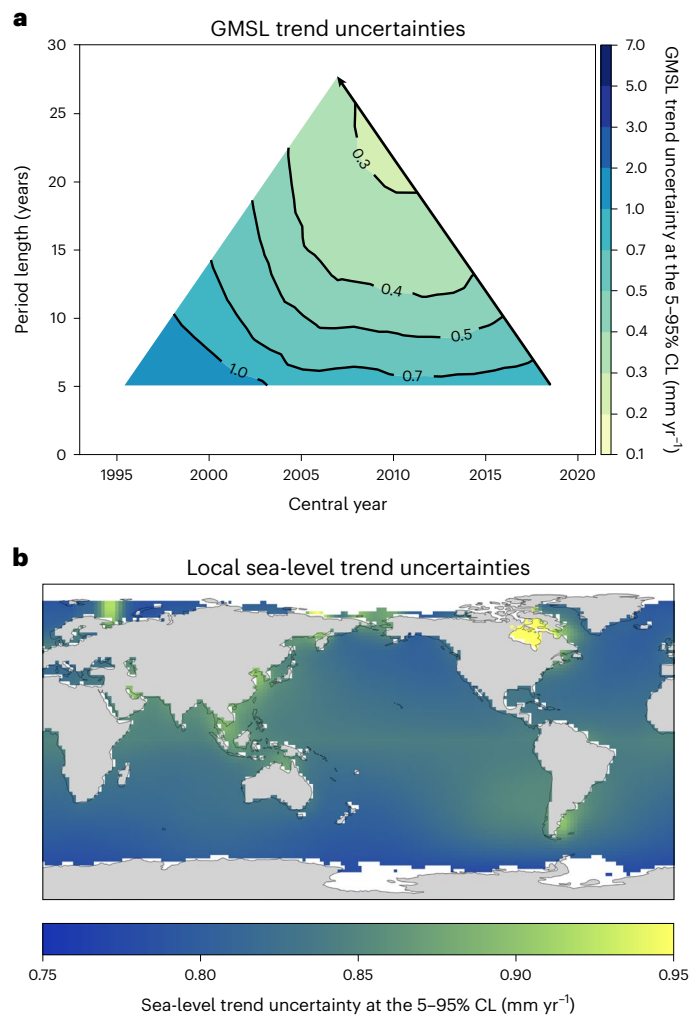


Fig. 2 | Sea-level trend uncertainties. **a**, Uncertainty in GMSL trends computed over any period longer than five years included in 1993–2020 (the central year of the period used to compute the trend is on the x axis, and the length of the period is on the y axis). **b**, Uncertainty in local sea-level trends over 1993–2019, as estimated in ref. 50. Panel **a** adapted with permission from ref. 49 under a Creative Commons license [CC BY 4.0](https://creativecommons.org/licenses/by/4.0/).

GMSL at all timescales from months to decades and for any metrics of sea level such as the rate of rise and the acceleration in sea level. On monthly timescales, GMSL uncertainty estimates show a decrease from an uncertainty of ±9 mm (90% CL) at the beginning of the record in 1993 to an uncertainty of ±3 mm (90% CL) close to the end of the record in 2015 (the record is the most accurate and precise in 2015 rather than at the end of the record in 2020 because in 2015 the estimate benefits from the correlated information of both the previous and the subsequent information contained in the record, while in 2020 the estimate only benefits from the correlated information of the previous information contained in the record) (Figs. 2a and 3).

The GMSL trend uncertainty is around ±0.7 mm yr⁻¹ (90% CL) for 10 yr trends and ±0.3 mm yr⁻¹ (90% CL) for the 28 yr trend (Fig. 2). In general, the uncertainty in sea-level trends decreases as the period of the trend calculation increases. This is because the different sources of noise in altimetry decorrelate on long timescales. Thus, for trends calculated over long periods, random noise averages out. Another effect is that the partitioning of the GMSL trend uncertainty among the different sources of error changes with timescales. For short trends (computed over 10 to 15 yr periods), the uncertainty due to the GMSL offset between TOPEX-A and TOPEX-B (which comes from changes in

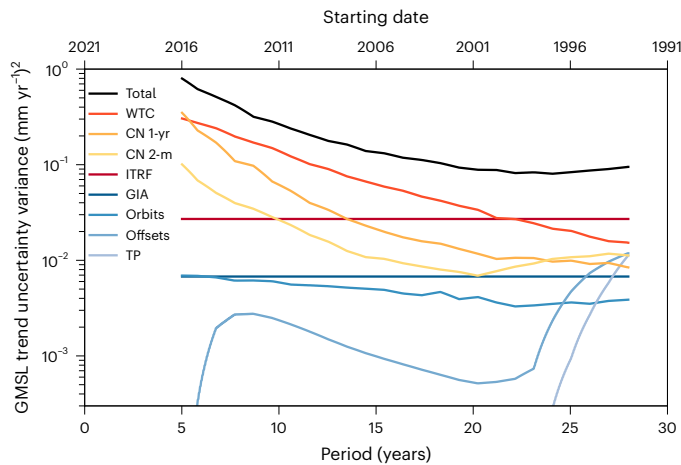


Fig. 3 | Partitioning of GMSL trend uncertainty sources. Uncertainties at the 66% CL in sea-level trends are computed over different periods that all end in 2020 (these correspond to the periods along the black arrow shown in Fig. 2a) and partitioning of the uncertainty among different sources: two-month and one-year correlated noises (CN 2-m and CN 1-yr, coming essentially from the radar altimeter errors), the radiometer WTC, the intermission offsets, the TOPEX drift (TP), the GIA and the ITRF (coming from errors in the ITRF realization). The same plot for acceleration is shown in Supplementary Fig. 4.

references in which the orbit and other geometrical parameters are expressed from one mission to another), the uncertainty due to the high-frequency correlated noise and the WTC uncertainty dominate. For long trends (computed over periods of 20 yr or more), systematic errors that are correlated at long timescales (such as WTC errors, glacial isostatic adjustment (GIA) errors or errors in the orbit induced by inaccuracy in the ITRF realization) tend to dominate (although they are small in amplitude; Fig. 3). Note that the date at which the trends are computed matters as well. Trends in GMSL are less accurate at the beginning of the record because of the poorer quality of TOPEX/Poseidon data than that of later altimeters. Regionally, the uncertainty in sea-level trends shows a spatial structure. Trends in sea level are the most reliable at high latitudes where the low-frequency correlated noise from the WTC is the smallest and far from the coast where the dynamical atmospheric correction and the tide correction are less uncertain (see an example with the 30 yr trend in local sea level in Fig. 2b; see also ref. 50). In terms of acceleration accuracy, the GMSL record shows pretty much the same spatiotemporal structure as for the trends (Supplementary Figs. 1–4).

Future needs in accuracy and precision

Compared with the beginning of the high-precision satellite altimetry era in the early 1990s, the improvement in terms of sea-level estimate precision and accuracy and in terms of the characterization of sea-level uncertainty and stability has been substantial. The current accuracy and precision enable us to close the sea-level budget with uncertainties that can be used to identify the causes of sea-level rise. The residual of the sea-level budget (that is, sea level minus thermal expansion and ocean mass changes) does not exceed ± 2 mm (90% CL) at interannual timescales (see, for example, Table 14 in ref. 18) and ± 0.3 mm yr⁻¹ (90% CL) for 20 yr and longer trends. This is within the uncertainty of Argo data, satellite gravimetry data and satellite altimetry data, confirming that the budget is closed and that ocean thermal expansion, glacier ice loss, Greenland ice loss and Antarctica ice loss explain 42%, 21%, 15% and 8%, respectively, of the GMSL rise since 1993 (Fig. 1a and ref. 18). The level of uncertainty in GMSL is also small enough to detect and attribute the part of current GMSL rise and acceleration that is due to anthropogenic GHG emissions^{51,52}, paving the way for the use of

Table 2 | Science questions and their needs in terms of the accuracy of sea-level estimates

Climate science question	Accuracy in GMSL rates (mm yr ⁻¹)	Accuracy in GMSL acceleration (mm yr ⁻¹ per decade)	Accuracy in regional sea-level rates (mm yr ⁻¹)
Closing the sea-level budget	Detection ^{a,b} : ± 0.1 Quantification ^{a,b} : ± 0.02	–	Detection ^{c,d} : ± 0.3 Quantification ^{c,d} : ± 0.07
Detecting and attributing the signal in sea level that is forced by GHG emissions	Detection ^{b,e} : ± 1.5 Quantification ^{b,e} : ± 0.7	–	Detection ^d : ± 0.5 Quantification ^d : ± 0.1
Estimating the EEI	Detection ^{d,f} : ± 0.1 Quantification ^{d,f} : ± 0.03	Detection ^{d,g} : ± 0.5 Quantification ^{d,g} : ± 0.1	

^aTo identify contributions from land water storage and deep ocean warming. ^bValues apply to 10 yr and longer periods. ^cTo identify the regional distribution of the contribution to sea level from land-ice melt. ^dValues apply to 20 yr and longer periods. ^eCalculated from ref. 51. These requirements are already met by the current altimetry observing system. ^fThese requirements correspond to the detection and quantification of decadal changes in the mean EEI on the order of ± 0.1 W m⁻². ^gThese requirements correspond to the detection and quantification of trends in the mean EEI on the order of ± 0.4 W m⁻² per decade.

satellite altimetry observations to constrain predictions and projections of future sea level⁵³.

But this level of uncertainty is still too large to identify small contributions to GMSL rise such as the exact contribution from land water storage or the deep ocean warming (depth > 2,000 m) not yet sampled by Argo. These two contributions are important to quantify. The first informs on the current trends of freshwater stocks, and the second informs on the current ocean heat uptake (OHU) and the capacity of the ocean to delay the effect of global warming on Earth's surface. Recent studies^{18,20,54,55} show that these contributions are currently around ± 0.2 mm yr⁻¹ (90% CL) on 20 yr and longer trends and should increase in the future. A simple rule of thumb is that a measurement's accuracy should be no worse than approximately 50% of the expected signal to detect it and 10% to quantify it⁴². An accuracy of ± 0.1 mm yr⁻¹ (90% CL) should therefore be enough to detect the small contributions of deep ocean warming and land water storage, and ± 0.02 mm yr⁻¹ (90% CL) should be enough to quantify them (Table 1).

At the regional scale, the situation is different. The regional sea-level signal at interannual and longer timescales is significantly larger in amplitude than at the global scale (typically in the range of -0.5 to 6 mm yr⁻¹ for 20 yr trends, for example). The local sea-level departures around the global mean are mostly explained by local departures in thermosteric sea level (that is the sea-level change due to thermal expansion^{56,57}) and salinity changes in high-latitude regions¹³, whereas the local sea-level departures induced by mass changes (that is, manometric sea-level changes) are much smaller and hardly detectable in observations. Indeed, manometric sea-level departures around the global mean typically amount to ± 0.7 mm yr⁻¹ (except very close to ice sheets⁵⁸), which is under the current local uncertainty in sea level (Fig. 2b). In addition, in several regions, including the mid to high latitudes and the Indian Ocean, the sea-level budget does not close locally by several millimetres per year (Supplementary Fig. 5 and refs. 59,60). This is more than 1 mm yr⁻¹ above the uncertainty of satellite altimetry (Fig. 2). If we apply the simple rule of thumb, we find that an uncertainty of ± 0.3 mm yr⁻¹ (or ± 0.07 mm yr⁻¹) for 20-year and longer trends is needed locally to detect (or quantify) the manometric sea-level departures around the global mean and close the sea-level budget (Table 2). To detect and quantify the local forced sea-level response to GHG emissions, the required level of uncertainty is similar. Climate models indicate that the locally forced response in sea level due to GHG emissions typically amounts to ± 1 mm yr⁻¹ on 20-year and longer

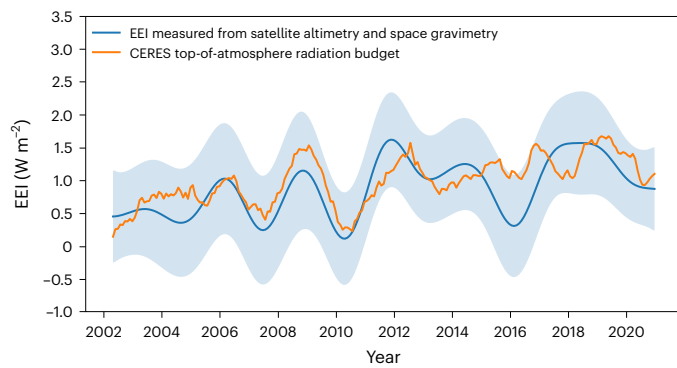


Fig. 4 | EEI from satellite altimetry and space gravimetry data compared with CERES observations. The blue line is the EEI derived from satellite altimetry and gravimetry data, called the geodetic estimate, with its 5–95% CL (blue shaded area). The orange line is the CERES estimate of the top-of-atmosphere radiation budget. The uncertainty in the mean of the CERES estimate and the mean of the geodetic estimate are respectively $\pm 2 \text{ W m}^{-2}$ and $\pm 0.2 \text{ W m}^{-2}$ at the 90% CL. Figure adapted with permission from ref. 65 under a Creative Commons license CC BY 4.0.

trends (Supplementary Fig. 6 and refs. 61,62), meaning that a local accuracy of $\pm 0.5 \text{ mm yr}^{-1}$ (or $\pm 0.1 \text{ mm yr}^{-1}$) on 20-year trends should be sufficient for detection (or quantification) of the regional forced response in sea level (Table 2).

The closure of the sea-level budget over the altimetry era has recently been used for another essential objective of climate science: estimating the EEI, which characterizes the radiative imbalance at the top of the atmosphere^{63–65}. The absolute value of the EEI quantifies the entire heat uptake of the climate system that is responsible for current climate change, making the EEI one of the most essential metrics that define the status of climate change⁶⁶. The EEI is about 0.5 W m^{-2} to 1 W m^{-2} (ref. 67). The Clouds and the Earth’s Radiant Energy System (CERES) project has been measuring the Earth’s radiative budget at the top of the atmosphere for several decades⁶⁷. The measurements are challenging, involving the incoming solar radiation, the scanning of outgoing radiation both visible and infrared, cloud cover, aerosols, and instrumental problems. The precision of the measurements is evaluated at the order of $\pm 0.17 \text{ W m}^{-2}$ (90% CL) at interannual timescales, but because of a potential bias of about $\pm 2 \text{ W m}^{-2}$, the accuracy is above $\pm 2 \text{ W m}^{-2}$ (ref. 67). The precision of CERES is sufficient to evaluate small changes in time of the EEI that are induced by natural or anthropogenic forcing^{68,69}. But the accuracy is not sufficient to estimate the mean EEI generated over the past few decades by anthropogenic GHG emissions. The best approach to estimating the mean EEI consists in estimating the excess of energy that is stored in the climate system in response to the EEI⁶³. Because about 91% of the excess of energy is stored in the ocean⁷⁰, the OHU is a precise proxy of the EEI. Today, the OHU can be derived with the highest accuracy, from in situ temperature measurements from Argo or from the thermal expansion estimated by the difference between satellite altimetry sea level and ocean mass from GRACE⁶³. Today, the current uncertainty in satellite altimetry sea-level rise and satellite gravimetry ocean mass trends enables us to derive the OHU with an uncertainty of $\pm 0.2 \text{ W m}^{-2}$ at the global scale over 15-year periods at the 90% CL (see Fig. 4 and refs. 64,65 for more details). At regional scales, preliminary results suggest an accuracy around $\pm 15 \text{ W m}^{-2}$ (equivalent top of the atmosphere) over 15-year periods for a resolution of $3^\circ \times 3^\circ$ (ref. 65). At decadal timescales, the EEI experiences changes on the order of $\pm 0.3 \text{ W m}^{-2}$ in response to climate internal modes such as the Pacific decadal oscillation⁷¹ and changes on the order of $\pm 0.1 \text{ W m}^{-2}$ in response to hiatuses such as the one experienced in the early 2000s⁶⁷. The EEI can also show trends on the order of $\pm 0.4 \text{ W m}^{-2}$ per decade in response to changes in

anthropogenic forcing^{68,69}. Monitoring these changes in the future with satellite altimetry and space gravimetry places new constraints on the satellite altimetry observing system. Using the expansion efficiency of heat in Table 1 shows that detecting (or quantifying) EEI decadal changes of $\pm 0.1 \text{ W m}^{-2}$ and trends of $\pm 0.4 \text{ W m}^{-2}$ per decade requires an uncertainty in sea level of $\pm 0.12 \text{ mm yr}^{-1}$ (or $\pm 0.03 \text{ mm yr}^{-1}$) for decadal trends and $\pm 0.5 \text{ mm yr}^{-1}$ per decade (or $\pm 0.1 \text{ mm yr}^{-1}$ per decade) for decadal accelerations.

Note that reaching this level of accuracy in the monitoring of the EEI on decadal timescales would bring another benefit: the capacity to monitor the physical climate system response to mitigation policies. With an uncertainty of $\pm 0.1 \text{ W m}^{-2}$ in observations of EEI decadal changes, climate model projections suggest that we can make the difference in terms of EEI response between an SSP1-2.6 scenario (with drastic GHG emission reduction) and an SSP5-8.5 scenario (business as usual) in less than two decades from now at the 66% CL. That is one decade earlier than with the monitoring of sea surface temperature (Supplementary Fig. 7).

Means of improvement

Space agencies are now preparing and launching the next generation of altimetry missions that will carry the future high-precision altimeters. These missions include synthetic aperture radar interferometers (that is, 2D imagers with high precision), such as SWOT, and classical nadir-looking altimeters (that is, 1D profilers with high accuracy), such as Sentinel topography next-generation missions. The interferometer of SWOT will yield 2D topography images with unprecedented precision^{72,73}, with the objective to observe smaller mesoscale or geoid features that classical nadir altimeters cannot resolve. However, the interferometer error budget is specified only for scales ranging from 15 to 1,000 km, and the instrument has no accuracy requirement for larger scales, let alone for long-term stability (that is, at seasonal to longer scales). SWOT may prove to be highly stable as TOPEX and Jason satellites did in their time, but it is too early to know. It will take years to determine the SWOT error budget at climate timescales and assess whether and how SWOT measurements are affected by instrumental and geophysical errors. In contrast, the Sentinel topography next-generation mission is designed to provide continuity of sea-level measurements with the same space and time resolution and the same accuracy and precision as current topography missions (including at large spatial scales and at climate timescales). Will that be enough to meet the future scientific needs in sea-level accuracy and precision?

Assuming the same error and uncertainty budget for the Sentinel next-generation altimetry missions as the current one, we find that continuity of sea-level measurements will not significantly reduce the uncertainty. This is because, after 20 years of record, the time correlation between errors vanishes, and the error budget is dominated by systematic errors (such as the WTC drift and the ITRF geocentre realization^{2,50}), which do not, at this point, decrease with time (Fig. 3). Some of these systematic errors are intrinsic to the measurement strategy. For example, the WTC stability could be reduced with improved microwave radiometer capabilities (such as more spectral channels, enhanced performance or longer calibration phases), although that would reduce the frequency of sea-level measurements. Other systematic errors are simply due to ancillary data errors such as the ITRF realization errors. In short, with the current estimated uncertainty in sea-level measurements and under the current design, the system capacity limits are close.

In the short term, there is still room for improvement in measurement and reducing uncertainty by working on the main sources of errors. For example, errors in the WTC can be reduced by cross-validating more often against available fundamental climate data records on atmospheric water vapour, which show significantly higher stability than on-board radiometer-based measurements⁷⁴. Preliminary tests show that this helps in detecting fast (within a year or so)

spurious drifts in the on-board radiometer-based WTC and reduces its uncertainty by up to 30%⁷⁵. The use of land-based transponders has proven to be very valuable in terms of quantifying and understanding range biases derived from the long time series of Jason-3 (and subsequently that of Sentinel-6 MF, since both follow the same orbit). This approach⁷⁶ can be used to isolate systematic and random constituents in the produced calibration results of the transponder (especially since other satellite altimeters including Cryosat-2, Sentinel-3A and Sentinel-3B also use the transponder system). Systematic components in the dispersion of transponder biases are identified as being of internal origin (coming from irregularities in the transponder instrument itself and its setting) and of external causes (arising from the altimeter, satellite orbit, geodynamic effects and so on). New efforts are piloting the use of ground-based passive corner reflectors as an independent check on transponder measurements⁷⁷.

Another efficient perspective is to improve the error characterization and the uncertainty estimates. At decadal and longer timescales, the sea-level budget is generally closed with a level of accuracy that is smaller than the level of uncertainty of altimetry, suggesting that the satellite altimetry system is actually more accurate than expected and that the uncertainty estimates are too conservative. A more rigorous and stringent estimate of uncertainties would better reflect the true performance of the altimetry system and give more confidence in the use of satellite altimetry to tackle the emerging questions identified in Table 2. The characterization of the error variance–covariance matrix of satellite altimetry has been the first step^{2,49,50}. The next step is to derive all errors and their spatiotemporal correlation from a propagation of the low-level instrumental errors down to the sea-level measurement. This is the objective of the ASELSU project of the European Space Agency.

In the longer term, to reduce the uncertainty in sea-level rise estimates, solutions should focus on improving the measurements of the WTC. For example, the stability of satellite altimeters' radiometers could be improved by changing calibration methods, developing new calibration strategies, extending the spatial and spectral capabilities of microwave radiometers, or fully exploiting GNSS-derived estimates of the WTC⁷⁸ or atmospheric model outputs⁷⁹. Also, solutions to reduce the ITRF realization uncertainty (and in particular the uncertainty in the geocentre drift) by increasing the number of satellite laser ranging stations around the world^{80–82} or by launching a geodetic mission with all precise positioning systems on the same platform, like the GENESIS space project⁸³, would be efficient. This would particularly improve the regional estimates of sea-level rise and variability, which are dominated by orbit errors.

A final important means of improvement is to take better advantage of the global sea-level budget and its relation to other observed global integrals of the Earth system, such as the ocean salinity⁸⁴, the sea ice volume⁸⁵, the top-of-atmosphere radiation budget⁶³, the Earth rotation or the true polar wander⁸⁶. All those global integrals are tightly linked together by the conservation laws of energy, mass and freshwater. Comparing them and testing their consistency would enable us to increase the built-in redundancy in the Earth observing system, which would further help control the stability of some observing sub-systems (such as satellite altimetry, the Argo network or the space gravimetry missions) and validate their uncertainty estimates. A recent example is the detection of a drift in the Jason-3 on-board radiometer and in Argo salinity with the non-closure of the sea-level budget^{34,87} and the poor closure of the global energy budget in 2016 (see also Fig. 4, updated from ref. 65). Another benefit of the built-in redundancy is that progress in the accuracy of a given observing sub-system can improve the accuracy on variables that were not targeted by this observing sub-system in the first place. A good example is the optimal estimate of the global water–energy cycle initiated by the National Aeronautics and Space Administration NEWS project^{88,89} and the GEWEX project of the World Climate Research Program⁹⁰. In these estimates, the accuracy of the

global water–energy cycle fluxes is objectively improved by bringing the observations together in a framework that conserves water and energy. The conservation laws tightly link observations and tend to reduce uncertainties by propagating to all the variables the constraint from the most accurate observed variables. To reap this benefit, sea-level observations should be routinely included in such frameworks, following the effort of Stephens et al.⁹⁰. A concrete estimate of how much improvement can be expected if these short-term and longer-term suggestions are actually realized shows that the GMSL detection levels in Table 2 would be reached at the 90% CL, and the quantification levels would be reached at the 66% CL (Supplementary Fig. 8).

Online content

Any methods, additional references, Nature Portfolio reporting summaries, source data, extended data, supplementary information, acknowledgements, peer review information; details of author contributions and competing interests; and statements of data and code availability are available at <https://doi.org/10.1038/s41558-023-01735-z>.

References

1. Legeais, J.-F. et al. An improved and homogeneous altimeter sea level record from the ESA Climate Change Initiative. *Earth Syst. Sci. Data* **10**, 281–301 (2018).
2. Ablain, M. et al. Uncertainty in satellite estimates of global mean sea-level changes, trend and acceleration. *Earth Syst. Sci. Data* **11**, 1189–1202 (2019).
3. BIPM *International Vocabulary of Metrology—Basic and General Concepts and Associated Terms (VIM)* 3rd edn (Joint Committee for Guides in Metrology, 2012); https://www.bipm.org/documents/20126/2071204/JCGM_200_2012.pdf/f0e1ad45-d337-bbeb-53a6-15fe649d0ff1
4. Palca, J. Ocean satellites: TOPEX launch comes closer. *Nature* **322**, 9 (1986).
5. Benveniste, J. & Bonnefond, P. Preface: 25 years of progress in radar altimetry. *Adv. Space Res.* <https://doi.org/10.1016/j.asr.2021.01.020> (2021).
6. Stammer, D. & Cazenave, A. *Satellite Altimetry over Oceans and Land Surfaces* (CRC, 2017).
7. Lambeck, K. Understanding ocean dynamics. *Nature* **373**, 474–475 (1995).
8. Fu, L.-L. & Cazenave, A. *Satellite Altimetry and Earth Sciences: A Handbook of Techniques and Applications* (Academic Press, 2001).
9. Stammer, D. Steric and wind-induced changes in TOPEX/POSEIDON large-scale sea surface topography observations. *J. Geophys. Res. Oceans* **102**, 20987–21009 (1997).
10. Cazenave, A. et al. Estimating ENSO influence on the global mean sea level, 1993–2010. *Mar. Geod.* **35**, 82–97 (2012).
11. Boening, C., Willis, J. K., Landerer, F. W., Nerem, R. S. & Fasullo, J. The 2011 La Niña: so strong, the oceans fell. *Geophys. Res. Lett.* <https://doi.org/10.1029/2012GL053055> (2012).
12. Fasullo, J. T., Boening, C., Landerer, F. W. & Nerem, R. S. Australia's unique influence on global sea level in 2010–2011. *Geophys. Res. Lett.* <https://doi.org/10.1002/grl.50834> (2013).
13. Hamlington, B. D., Frederikse, T., Nerem, R. S., Fasullo, J. T. & Adhikari, S. Investigating the acceleration of regional sea level rise during the satellite altimeter era. *Geophys. Res. Lett.* **47**, e2019GL086528 (2020).
14. Cazenave, A. Sea level and volcanoes. *Nature* **438**, 35–36 (2005).
15. Church, J. A., White, N. J. & Arblaster, J. M. Significant decadal-scale impact of volcanic eruptions on sea level and ocean heat content. *Nature* **438**, 74–77 (2005).
16. Grinsted, A., Moore, J. C. & Jevrejeva, S. Observational evidence for volcanic impact on sea level and the global water cycle. *Proc. Natl Acad. Sci. USA* **104**, 19730–19734 (2007).

17. Cazenave, A. et al. The rate of sea-level rise. *Nat. Clim. Change* **4**, 358–361 (2014).
18. WCRP Global Sea Level Budget Group. Global sea-level budget 1993–present. *Earth Syst. Sci. Data* **10**, 1551–1590 (2018).
19. Frederikse, T. et al. The causes of sea-level rise since 1900. *Nature* **584**, 393–397 (2020).
20. Llovel, W., Willis, J. K., Landerer, F. W. & Fukumori, I. Deep-ocean contribution to sea level and energy budget not detectable over the past decade. *Nat. Clim. Change* **4**, 1031–1035 (2014).
21. Chen, X. et al. The increasing rate of global mean sea-level rise during 1993–2014. *Nat. Clim. Change* **7**, 492–495 (2017).
22. Horwath, M. et al. Global sea-level budget and ocean-mass budget, with focus on advanced data products and uncertainty characterisation. *Earth Syst. Sci. Data* **14**, 411–447 (2022).
23. Roemmich, D. et al. The Argo program: observing the global ocean with profiling floats. *Oceanography* **22**, 34–43 (2009).
24. Tapley, B. D. et al. Contributions of GRACE to understanding climate change. *Nat. Clim. Change* **9**, 358–369 (2019).
25. Wong, A. P. S. et al. Argo data 1999–2019: two million temperature–salinity profiles and subsurface velocity observations from a global array of profiling floats. *Front. Mar. Sci.* **7**, 700 (2020).
26. Roemmich, D. & Gilson, J. The 2004–2008 mean and annual cycle of temperature, salinity, and steric height in the global ocean from the Argo program. *Prog. Oceanogr.* **82**, 81–100 (2009).
27. Abraham, J. P. et al. A review of global ocean temperature observations: implications for ocean heat content estimates and climate change. *Rev. Geophys.* **51**, 450–483 (2013).
28. Wouters, B. et al. GRACE, time-varying gravity, Earth system dynamics and climate change. *Rep. Prog. Phys.* **77**, 116801 (2014).
29. Blazquez, A. et al. Exploring the uncertainty in GRACE estimates of the mass redistributions at the Earth surface: implications for the global water and sea level budgets. *Geophys. J. Int.* **215**, 415–430 (2018).
30. Uebbing, B., Kusche, J., Rietbroek, R. & Landerer, F. W. Processing choices affect ocean mass estimates from GRACE. *J. Geophys. Res. Oceans* **124**, 1029–1044 (2019).
31. Landerer, F. W. et al. Extending the global mass change data record: Grace follow-on instrument and science data performance. *Geophys. Res. Lett.* <https://doi.org/10.1029/2020GL088306> (2020).
32. Leuliette, E. W. & Willis, J. K. Balancing the sea level budget. *Oceanography* <https://doi.org/10.5670/oceanog.2011.32> (2011).
33. Amin, H., Bagherbandi, M. & Sjöberg, L. Quantifying barostatic sea-level change from satellite altimetry, GRACE and Argo observations over 2005–2016. *Adv. Space Res.* **65**, 1922–1940 (2020).
34. Barnoud, A. et al. Contributions of altimetry and Argo to non-closure of the global mean sea level budget since 2016. *Geophys. Res. Lett.* **48**, e2021GL092824 (2021).
35. Beckley, B. D., Callahan, P. S., Hancock III, D. W., Mitchum, G. T. & Ray, R. D. On the ‘cal-mode’ correction to TOPEX satellite altimetry and its effect on the global mean sea level time series. *J. Geophys. Res. Oceans* **122**, 8371–8384 (2017).
36. Dieng, H. B., Cazenave, A., Meyssignac, B. & Ablain, M. New estimate of the current rate of sea level rise from a sea level budget approach. *Geophys. Res. Lett.* **44**, 3744–3751 (2017).
37. Watson, C. S. et al. Unabated global mean sea-level rise over the satellite altimeter era. *Nat. Clim. Change* **5**, 565–568 (2015).
38. Chenal, J., Meyssignac, B., Ribes, A. & Guillaume-Castel, R. Observational constraint on the climate sensitivity to atmospheric CO₂ concentrations changes derived from the 1971–2017 global energy budget. *J. Clim.* **35**, 4469–4483 (2022).
39. Meyssignac, B., Chenal, J., Loeb, N., Guillaume-Castel, R. & Ribes, A. Time-variations of the climate feedback parameter λ are associated with the Pacific Decadal Oscillation. *Commun. Earth Environ.* **4**, 241 (2023).
40. Balmaseda, M. A., Mogensen, K. & Weaver, A. T. Evaluation of the ECMWF ocean reanalysis system ORAS4. *Q. J. R. Meteorol. Soc.* <https://doi.org/10.1002/qj.2063> (2013).
41. Balmaseda, M. A., Trenberth, K. E. & Källén, E. Distinctive climate signals in reanalysis of global ocean heat content. *Geophys. Res. Lett.* **40**, 1754–1759 (2013).
42. Wunsch, C. Global ocean integrals and means, with trend implications. *Annu. Rev. Mar. Sci.* **8**, 1–33 (2016).
43. Donlon, C. J. et al. The Copernicus Sentinel-6 mission: enhanced continuity of satellite sea level measurements from space. *Remote Sens. Environ.* **258**, 112395 (2021).
44. Donlon, C. et al. The Global Monitoring for Environment and Security (GMES) Sentinel-3 mission. *Remote Sens. Environ.* **120**, 37–57 (2012).
45. Henry, O. et al. Effect of the processing methodology on satellite altimetry-based global mean sea level rise over the Jason-1 operating period. *J. Geod.* **88**, 351–361 (2014).
46. Scharffenberg, M. G. & Stammer, D. Time–space sampling-related uncertainties of altimetric global mean sea level estimates. *J. Geophys. Res. Oceans* **124**, 7743–7755 (2019).
47. Ballarotta, M. et al. On the resolutions of ocean altimetry maps. *Ocean Sci.* **15**, 1091–1109 (2019).
48. Rieu, P. et al. Exploiting the Sentinel-3 tandem phase dataset and azimuth oversampling to better characterize the sensitivity of SAR altimeter sea surface height to long ocean waves. *Adv. Space Res.* **67**, 253–265 (2021).
49. Guérou, A. et al. Current observed global mean sea level rise and acceleration estimated from satellite altimetry and the associated measurement uncertainty. *Ocean Sci.* **19**, 431–451 (2023).
50. Prandi, P. et al. Local sea level trends, accelerations and uncertainties over 1993–2019. *Sci. Data* **8**, 1 (2021).
51. Slangen, A. B. A. et al. Anthropogenic forcing dominates global mean sea-level rise since 1970. *Nat. Clim. Change* **6**, 701–705 (2016).
52. Nerem, R. S. et al. Climate-change–driven accelerated sea-level rise detected in the altimeter era. *Proc. Natl Acad. Sci. USA* **115**, 2022–2025 (2018).
53. Nerem, R. S., Frederikse, T. & Hamlington, B. D. Extrapolating empirical models of satellite-observed global mean sea level to estimate future sea level change. *Earths Future* **10**, e2021EF002290 (2022).
54. Purkey, S. G. & Johnson, G. C. Warming of global abyssal and deep southern ocean waters between the 1990s and 2000s: contributions to global heat and sea level rise budgets. *J. Clim.* **23**, 6336–6351 (2010).
55. Desbruyères, D. G., Purkey, S. G., McDonagh, E. L., Johnson, G. C. & King, B. A. Deep and abyssal ocean warming from 35 years of repeat hydrography. *Geophys. Res. Lett.* **43**, 10356–10365 (2016).
56. Forget, G. & Ponte, R. M. The partition of regional sea level variability. *Prog. Oceanogr.* <https://doi.org/10.1016/j.pocean.2015.06.002> (2015).
57. Meyssignac, B. et al. Causes of the regional variability in observed sea level, sea surface temperature and ocean colour over the period 1993–2011. *Surv. Geophys.* <https://doi.org/10.1007/s10712-016-9383-1> (2016).
58. Hsu, C.-W. & Velicogna, I. Detection of sea level fingerprints derived from GRACE gravity data. *Geophys. Res. Lett.* **44**, 8953–8961 (2017).
59. Rietbroek, R., Brunnabend, S.-E., Kusche, J., Schröter, J. & Dahle, C. Revisiting the contemporary sea-level budget on global and regional scales. *Proc. Natl Acad. Sci. USA* **113**, 1504–1509 (2016).

60. Royston, S. et al. Can we resolve the basin-scale sea level trend budget from GRACE ocean mass? *J. Geophys. Res. Oceans* **125**, e2019JC015535 (2020).
61. Fasullo, J. T. & Nerem, R. S. Altimeter-era emergence of the patterns of forced sea-level rise in climate models and implications for the future. *Proc. Natl Acad. Sci. USA* **115**, 12944–12949 (2018).
62. Bilbao, R. A. F., Gregory, J. M. & Bouttes, N. Analysis of the regional pattern of sea level change due to ocean dynamics and density change for 1993–2009 in observations and CMIP5 AOGCMs. *Clim. Dyn.* **45**, 2647–2666 (2015).
63. Meyssignac, B. et al. Measuring global ocean heat content to estimate the Earth energy imbalance. *Front. Mar. Sci.* <https://doi.org/10.3389/fmars.2019.00432> (2019).
64. Hakuba, M. Z., Frederikse, T. & Landerer, F. W. Earth's energy imbalance from the ocean perspective (2005–2019). *Geophys. Res. Lett.* **48**, e2021GL093624 (2021).
65. Marti, F. et al. Monitoring the ocean heat content change and the Earth energy imbalance from space altimetry and space gravimetry. *Earth Syst. Sci. Data* **14**, 229–249 (2022).
66. von Schuckmann, K. et al. An imperative to monitor Earth's energy imbalance. *Nat. Clim. Change* **6**, 138–144 (2016).
67. Loeb, N. G. et al. Clouds and the Earth's Radiant Energy System (CERES) Energy Balanced and Filled (EBAF) Top-of-Atmosphere (TOA) Edition-4.0 data product. *J. Clim.* **31**, 895–918 (2018).
68. Loeb, N. G. et al. Satellite and ocean data reveal marked increase in Earth's heating rate. *Geophys. Res. Lett.* **48**, e2021GL093047 (2021).
69. Raghuraman, S. P., Paynter, D. & Ramaswamy, V. Anthropogenic forcing and response yield observed positive trend in Earth's energy imbalance. *Nat. Commun.* **12**, 4577 (2021).
70. von Schuckmann, K. et al. Heat stored in the Earth system: where does the energy go? *Earth Syst. Sci. Data* **12**, 2013–2041 (2020).
71. Loeb, N. G., Thorsen, T. J., Norris, J. R., Wang, H. & Su, W. Changes in Earth's energy budget during and after the 'pause' in global warming: an observational perspective. *Climate* **6**, 62 (2018).
72. Desai, S. *Surface Water and Ocean Topography Mission (SWOT) Project Science Requirements Document Technical Report JPL D-61923, Rev. B (JPL, 2018)*; https://swot.jpl.nasa.gov/system/documents/files/2176_2176_D-61923_SRD_Rev_B_20181113.pdf
73. Esteban-Fernandez, D. *SWOT Mission Performance and Error Budget Technical Report JPL D-79084, Rev. A (NASA/JPL, 2017)*; https://swot.jpl.nasa.gov/system/documents/files/2178_2178_SWOT_D-79084_v10Y_FINAL_REVA_06082017.pdf
74. Schröder, M. et al. The GEWEX Water Vapor Assessment archive of water vapour products from satellite observations and reanalyses. *Earth Syst. Sci. Data* **10**, 1093–1117 (2018).
75. Barnoud, A. et al. Reducing the uncertainty in the satellite altimetry estimates of global mean sea level trends using highly stable water vapor climate data records. *J. Geophys. Res. Oceans* **128**, e2022JC019378 (2023).
76. Mertikas, S. P. et al. Performance evaluation of the CDN1 altimetry Cal/Val transponder to internal and external constituents of uncertainty. *Adv. Space Res.* **70**, 2458–2479 (2022).
77. Gibert, F. et al. A trihedral corner reflector for radar altimeter calibration. *IEEE Trans. Geosci. Remote Sens.* **61**, 5101408 (2023).
78. Fernandes, M. J., Lázaro, C. & Vieira, T. On the role of the troposphere in satellite altimetry. *Remote Sens. Environ.* **252**, 112149 (2021).
79. Vieira, T., Fernandes, M. J. & Lázaro, C. An enhanced retrieval of the wet tropospheric correction for Sentinel-3 using dynamic inputs from era5. *J. Geod.* **96**, 28 (2022).
80. Kehm, A., Blossfeld, M., König, P. & Seitz, F. Future TRFs and GGOS—where to put the next SLR station? *Adv. Geosci.* **50**, 17–25 (2019).
81. Arnold, D., Montenbruck, O., Hackel, S. & Sosnica, K. Satellite laser ranging to low Earth orbiters: orbit and network validation. *J. Geod.* **93**, 2315–2334 (2019).
82. Otsubo, T. et al. Effective expansion of satellite laser ranging network to improve global geodetic parameters. *Earth Planets Space* **68**, 65 (2016).
83. Delva, P. et al. GENESIS: co-location of geodetic techniques in space. *Earth Planets Space* **75**, 5 (2023).
84. Llovel, W. et al. Global ocean freshening, ocean mass increase and global mean sea level rise over 2005–2015. *Sci. Rep.* **9**, 17717 (2019).
85. Munk, W. Ocean freshening, sea level rising. *Science* **300**, 2041–2043 (2003).
86. Mitrovica, J. X. et al. Reconciling past changes in Earth's rotation with 20th century global sea-level rise: resolving Munk's enigma. *Sci. Adv.* **1**, e1500679 (2015).
87. Barnoud, A. et al. Revisiting the global mean ocean mass budget over 2005–2020. *Ocean Sci.* **19**, 321–334 (2023).
88. L'Ecuyer, T. S. et al. The observed state of the energy budget in the early twenty-first century. *J. Clim.* **28**, 8319–8346 (2015).
89. Rodell, M. et al. The observed state of the water cycle in the early twenty-first century. *J. Clim.* **28**, 8289–8318 (2015).
90. Stephens, G. et al. The first 30 years of GEWEX. *Bull. Am. Meteorol. Soc.* <https://doi.org/10.1175/BAMS-D-22-0061.1> (2022).
91. Taburet, G., Mertz, F. & Legeais, J.-F. *Product User Guide and Specification: Sea Level ECMWF Copernicus Report (CLS, 2021)*.

Publisher's note Springer Nature remains neutral with regard to jurisdictional claims in published maps and institutional affiliations.

Springer Nature or its licensor (e.g. a society or other partner) holds exclusive rights to this article under a publishing agreement with the author(s) or other rightsholder(s); author self-archiving of the accepted manuscript version of this article is solely governed by the terms of such publishing agreement and applicable law.

© Springer Nature Limited 2023

Methods

Sea-level estimates at regional and global scales from satellite altimetry

Sea-level estimates at regional scales are derived from the sea-level products operationally generated by C3S. This dataset, fully described in ref. 92, is dedicated to sea-level stability for climate applications. It provides daily sea-level anomaly grids at 1/4° spatial resolution from January 1993 to August 2021, based at any given time on a reference altimeter mission (TOPEX/Poseidon, Jason-1,2,3 and soon S6-MF), plus a complementary mission (ERS-1,2, Envisat, Cryosat and SARAL/AltiKa) to increase the spatial coverage. To measure the current climate-related contribution to regional sea-level rise, sea-level estimates must be corrected for the GIA effect using a model^{93,94} and for the deformations of the ocean bottom in response to modern melt of land ice^{95,96}. The C3S sea-level grids must also be corrected for a time-varying instrumental drift on the TOPEX altimeter (side A) from 1993 to 1999¹⁸. Sea-level estimates at the global scale are calculated from a global weighted mean (taking into account the surface of the cells) of C3S corrected sea-level grids. An alternative approach is to use the AVISO GMSL time series, which contains similar sea-level estimates at the global scale⁴⁹.

Error and uncertainty budget estimate and variance–covariance matrix computation at global and regional scales

An error and uncertainty budget of the GMSL time series is provided in ref. 2 and was recently updated in ref. 49. The budget contains the main source of errors impacting the GMSL stability accuracy. Different types of errors are provided, such as inter-mission GMSL offset, correlated errors at different timescales (typically two months, one year and five years due to altimeter parameters, geophysical corrections, WTC and orbit) and linear drifts (due to orbit, ITRF and GIA). The budget also provides the uncertainty description of each error (for example, time-correlated scale and standard deviation) and the statistical model applied (for example, Gaussian attenuation model). The individual variance–covariance matrix (Σ_i) of each error source is then calculated from a large number of random draws of the simulated error signal with a standard normal distribution. Assuming individual matrices (Σ_i) are independent, they are summed together to build the GMSL error variance–covariance matrix (Supplementary Fig. 9). At regional scales, a similar approach was developed in ref. 50. The regional sea-level error and uncertainty budget is described at regional scales. The description of errors and their uncertainty characterization is used to create a map of the standard deviation for some errors (high-frequency noise from orbit determination and geophysical corrections, low-frequency noise from the WTC and drift from the GIA correction). The variance–covariance matrix of regional sea-level errors is derived from the regional budget in the same way as at the global scale. At regional scales, the matrix describes the error covariance of each regional sea-level time series individually. To date, the spatial correlation of regional sea-level errors has not been described.

Uncertainty estimates in sea-level trends and acceleration and breakdown into components

From the error variance–covariance matrix (Σ), the sea-level trend and acceleration uncertainties can be estimated for any time span included in the altimeter period (1993–2021) at both global and regional scales (Fig. 2 and Supplementary Figs. 2 and 3). The mathematical formalism applied is fully described in ref. 2. It basically consists in fitting the trend or the acceleration from a linear regression model ($y = X\beta + \epsilon$) applying an ordinary least squares approach where the estimator of β , denoted $\hat{\beta}$, is:

$$\hat{\beta} \approx (X^T X)^{-1} X^T y$$

and where the distribution of the estimator takes into account Σ and follows a normal law:

$$\hat{\beta} \sim N(\beta, (X^T X)^{-1} (X^T \Sigma X) (X^T X)^{-1})$$

The trend and acceleration uncertainties of each component of the sea-level error budget can be estimated by the same method by choosing as input the corresponding individual variance–covariance matrix (Σ_i). This allows us to separate the contribution of each error to the total sea-level uncertainties in trends (Fig. 3) and acceleration (Supplementary Fig. 4).

References

92. Legeais, J.-F. et al. Copernicus sea level space observations: a basis for assessing mitigation and developing adaptation strategies to sea level rise. *Front. Mar.* **8**, 704721 (2021).
93. Peltier, W. Global glacial isostasy and the surface of the ice-age Earth: the ICE-5G (VM2) model and GRACE. *Annu. Rev. Earth Planet. Sci.* **32**, 111–149 (2004).
94. Spada, G. & Melini, D. SELEN⁴ (SELEN version 4.0): a Fortran program for solving the gravitationally and topographically self-consistent sea-level equation in glacial isostatic adjustment modeling. *Geosci. Model Dev.* **12**, 5055–5075 (2019).
95. Frederikse, T., Riva, R. E. M. & King, M. A. Ocean bottom deformation due to present-day mass redistribution and its impact on sea level observations. *Geophys. Res. Lett.* **44**, 12306–12314 (2017).
96. Lickley, M. J., Hay, C. C., Tamisiea, M. E. & Mitrovica, J. X. Bias in estimates of global mean sea level change inferred from satellite altimetry. *J. Clim.* **31**, 5263–5271 (2018).

Acknowledgements

This work was partially supported by the European Space Agency (ESA) Analysis of the Uncertainty of the Stability of the Altimeter Measurement of Sea Level Rise (ASELSU) study contract no. 4000135959/21/NL/AD. It was also partially supported by the ESA Climate Change Initiative sea-level budget closure (phase 2) project. This work was supported by the Centre National d'Etudes Spatiales, with a focus on Sentinel 6/MF.

Author contributions

B.M. led and conducted the study and wrote most of the manuscript. M.A., A.G. and P.P. participated in the writing of the Methods. M.A., A.G., P.P., A. Barnoud, A. Blazquez, S.F. and V.R. contributed to the data processing and figure generation. All authors contributed to scientific and technical discussions and read and approved the content of the manuscript.

Competing interests

The authors declare no competing interests.

Additional information

Supplementary information The online version contains supplementary material available at <https://doi.org/10.1038/s41558-023-01735-z>.

Correspondence should be addressed to Benoit Meyssignac.

Peer review information *Nature Climate Change* thanks Mohammad Bagherbandi, Abdul-Lateef Balogun and Florian Seitz for their contribution to the peer review of this work.

Reprints and permissions information is available at www.nature.com/reprints.